Self-assembly of polymer-encased lipid nanodiscs and membrane protein reconstitution

Bikash R. Sahoo[†], Takuya Genjo[†], Kanhu C. Maharana[‡], Ayyalusamy Ramamoorthy[*†]

† Biophysics and Department of Chemistry, University of Michigan,

Ann Arbor, MI 48109, USA

‡ Department of Bioinformatics, Orissa University of Agriculture and Technology,

Odisha, 751003, India

Corresponding Author

*E-mail: ramamoor@umich.edu

ABSTRACT: The absence of detergent and curvature makes nanodiscs to be excellent membrane mimetics. The lack of structural and mechanistic model of polymer-encapsulated lipid-nanodiscs limits their use to study the structure, dynamics and function of membrane proteins. In this study, we parametrized and optimized the coarse-graining (CG) bead-mapping for two differently charged and functionalized copolymers, namely styrene-maleic acid (SMA-EA) and polymethacrylate (PMA-QA), for the *Martini* force-field framework and showed nanodisc formation (< 8 nm diameter) on a time scale of tens of microseconds using molecular dynamics (MD) simulation. Structural models of ~ 2.0 or 4.8 kDa PMA-QA and ~2.2 kDa SMA-EA polymer based lipid-nanodiscs highlights the importance of polymer chemical structure, size and polymer:lipid molar ratio in the optimization of nanodisc structure. The ideal spatial arrangement of polymers in nanodisc, nanodisc size and thermal stability obtained from our MD simulation correlates well with the experimental observations. The polymer-nanodisc were tested for the reconstitution of single-pass or multi-pass transmembrane proteins. We expect this study to be useful in the development of novel polymer based lipid-nanodiscs and for the structural studies of membrane proteins.

TOC GRAPHICS

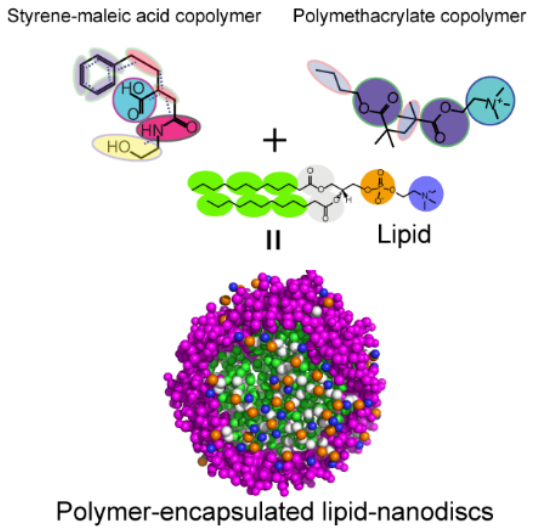

KEYWORDS Styrene-maleic acid copolymer; Polymethacrylate copolymers; Nanodisc; Molecular dynamics simulation; Coarse-grained; Membrane protein reconstitution.

Despite the recent advances in structural biology, membrane proteins continue to pose challenges to most biophysical techniques and biochemical approaches.[1,2] The aggregation kinetics of membrane proteins outside lipid membrane[3] impulse researchers to develop methods to study their native structures[4]. As a result, reconstitution of membrane proteins using membrane mimetics such as bicelles, micelles, liposomes or nanodiscs[4] has significantly eased the interrogation of membrane-associated proteins. Particularly, there is considerable interest in the development and application of nanodiscs[5,6]. Use of nanodiscs as a potential nanomedicine for protein misfolded diseases like Alzheimer's disease is bound to create avenues for exciting biomedical applications[7–9]. These nanodiscs provide a detergent-free native-like lipid bilayer environment for functional reconstitution of a membrane protein or protein-protein complex. In addition, the size-tunable and lipid selectivity properties of nanodiscs have enabled researchers to design membrane protein selective nanodiscs for structural and functional studies[10].

Recent studies have demonstrated the advantages of polymer based nanodiscs[11,12] that include extraction of membrane proteins directly from cells, tolerance against pH and divalent metal ions, size tunability by simply changing lipid:polymer ratio, formation of macro-nanodiscs and their magnetic-alignment, and feasibility of applying biophysical techniques including solution and solid-state NMR experiments. We have also demonstrated the use of polymer based nanodiscs for the investigation of amyloid peptide interaction with lipid membrane at molecular level.[13] In spite of the success, there are several disadvantages that need to be overcome for a wide spread application of polymer based nanodiscs. For example, the amphiphilic polymer has been shown to interact with the membrane protein of interest, which can interfere with folding and induce non-native conformational changes[14]. Synthetic modifications have been demonstrated to overcome some of these limitations. However, there is a lack of understanding of spontaneous

nanodisc formation by copolymers at atomistic scale. Such information would enable the design of better suited polymer and polymer nanodisc for structural and functional investigation of a given membrane protein. While real-time monitoring of the self-assembly process to form nanodisc at atomic resolution is challenging, here we report a CG molecular dynamics (MD) simulation approach and demonstrate its use to understand the formation of nanodiscs. Specifically, parametrization and optimization of two functionally different copolymers, namely SMA-EA and PMA-QA, and their ability to self-assemble with lipids to form polymer nanodiscs are reported for the first time. Reconstitutions of three different membrane proteins (bacterial sensory rhodopsin (srII), amyloid precursor protein's (APP) transmembrane domain and integrin-β3)[15–17] in these polymer nanodiscs are also demonstrated at atomic scale using microsecond timescale CG MD simulations.

Parameterization and construction of CG models to perform MD simulation using SMA-EA (2.2 kDa) and PMA-QA (2.0 kDa or 4.8 kDa) polymers are shown in Figure 1. CG bead mapping was accomplished based on experimentally identified functional groups (styrene, $-N^+R_3$, COO^-) that are crucial for the nanodisc formation by the polymers.[18,19] The pseudo-bonds and bond lengths were determined from all-atom topology of the respective polymer (Fig. 1). Two differently sized PMA-QA (~2.0 kDa and ~4.8 kDa) were tested with a similar CG bead mapping to understand the role of polymer length in the formation of nanodiscs. In addition, we employed two different lipids to evaluate the suitability of lipids for the nanodisc formation: zwitterionic lipid DLPC (1,2-dimyristoyl-sn-glycero-3-phosphocholine) and anionic lipid DLPS (1,2-dilauroyl-sn-glycero-3-phospho-L-serine).

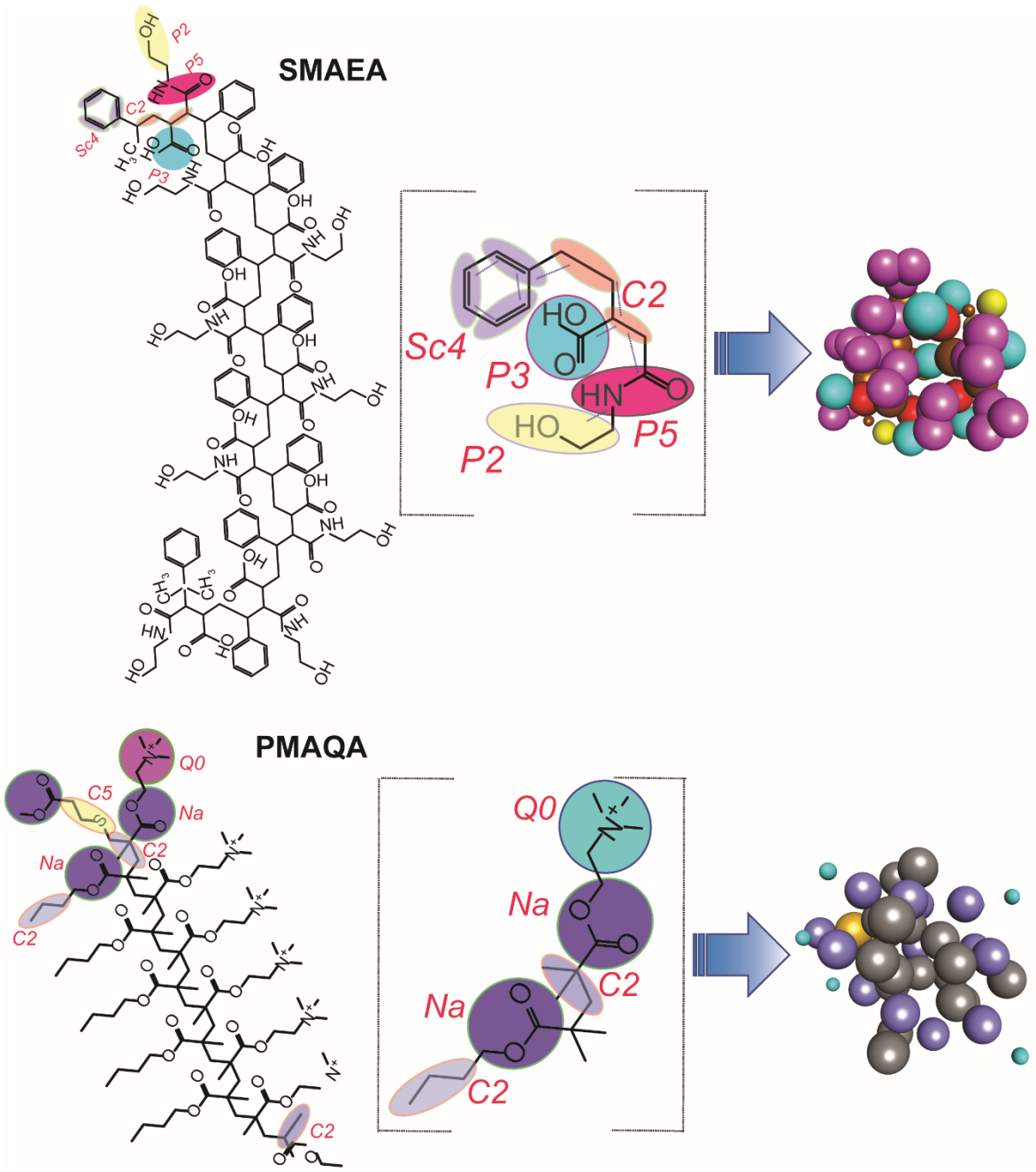

Figure 1. Coarse-grained (CG) mapping for the parameterization of SMA-EA and PMA-QA nanodisc forming copolymers. Chemical structures of SMA-EA (top left) and PMA-QA (bottom left) were built using *ChemDraw*. The selected CG groups are high-lighted in colors (middle column), and the CG bead mapping of each repeated units in SMA-EA or PMA-QA and their corresponding CG-models are shown in the right-most panel.

The solubilization of lipid-bilayers by a polymer has been shown to generate discoidal nanodiscs by light scattering, TIRF fluorescence and NMR experiments[18,19]. Under the experimental

conditions, such morphological transition happens spontaneously and sometimes require mechanical procedures such as repeated freeze and thaw cycles depending on the lipid composition[18,19]. Here, we investigate such a transition using a DLPC lipid bilayer model in Martini force field[20]. As illustrated in Figure S1, SMA-EA was found to substantially destabilize the DLPC lipid bilayer (SMA-EA:DLPC=1:4) over a time period of 4 μS MD simulation. The self-assembly of SMA-EA on the DLPC lipid-bilayer facilitates membrane insertion and pore formation by SMA-EA within ~ 2 μs. Segregation of upper and lower leaflet lipids with centrally bridged SMA-EA were identified at the end of 4 μS MD simulation (Fig. S1). Such membrane destabilization and transient pore formation by SMA copolymer (~7.4 kDa) was recently reported.[21] Even though SMA-EA disrupts DLPC lipid bilayer, we did not observe nanodisc formation within the microsecond timescale of MD simulation mentioned above. Therefore, these findings suggest that a longer timescale of MD simulation is essential to achieve sufficient disruption of the pre-structured lipid bilayer by the polymer to form a discoidal nanodisc as reported from experimental studies.

In order to overcome the limitation mentioned above, we next performed MD simulation to monitor the spontaneous assembly of randomly distributed polymer (SMA-EA or PMA-QA) and free DLPC lipids in solution at 1:4 polymer:DLPC molar ratio. Remarkably, the randomly distributed polymers and DLPC lipids in aqueous solution exhibited the formation of discoidal shape nanodiscs within 10 μs simulation. PMA-QA and SMA-EA copolymers with nearly equivalent size (~2.0 kDa), but differing in hydrophobic and hydrophilic functionalization, generated nanodiscs of size ~7.0 and 7.5 nm, respectively (Fig. 2). The polymers were found to be

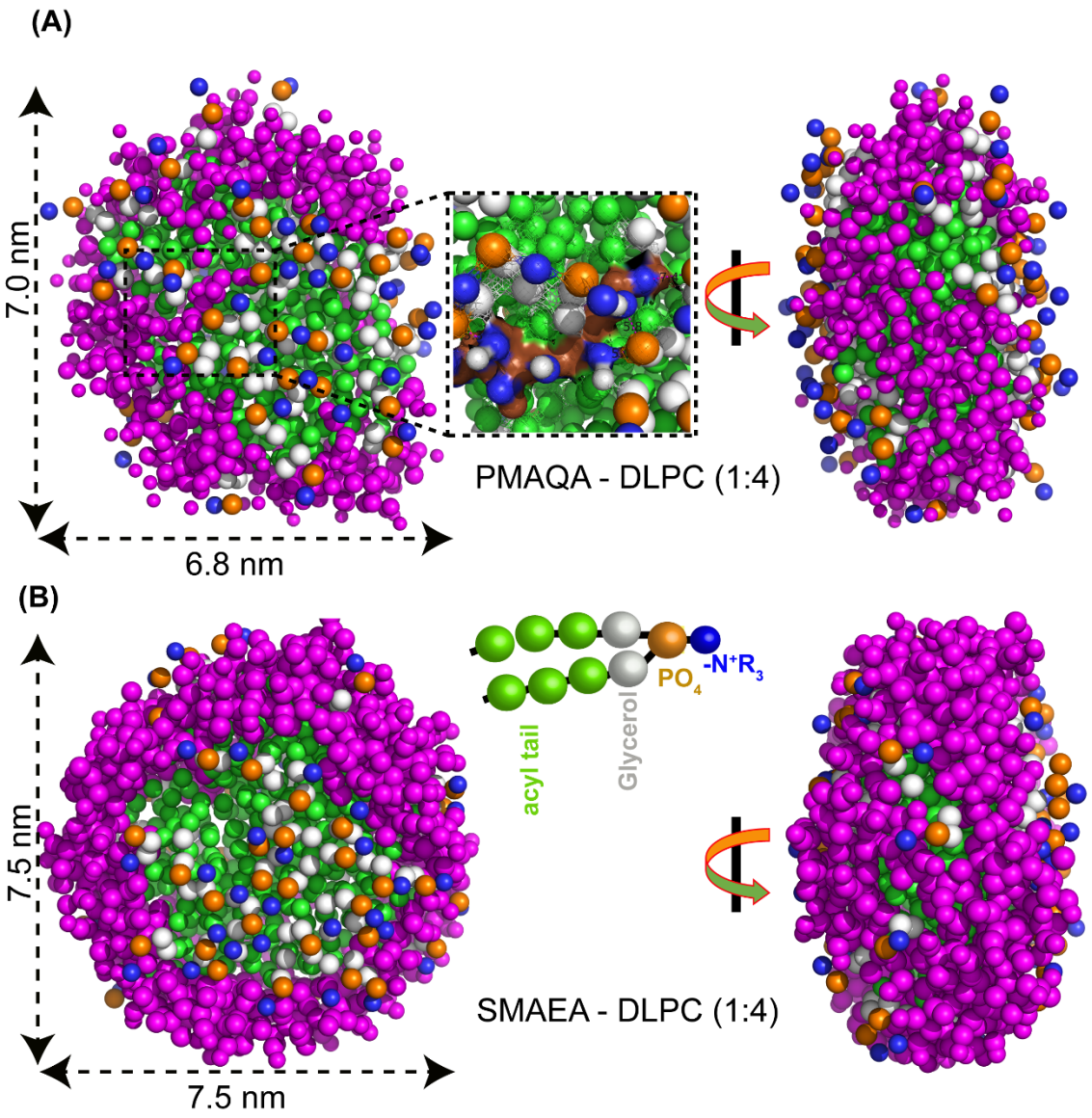

Figure 2. Coarse-grained MD simulation showing the spontaneous formation of DLPC nanodiscs on a time scale of 10 μs. MD snapshots shows discoidal DLPC nanodiscs encased by PMA-QA (A) or SMA-EA (B) at 1:4 polymer:lipid molar ratio; top-down (left) and side (right) views. The double-headed arrow indicates the average diameter of the nanodisc. The polymers are shown in violet and CG atoms of DLPC in other colors. Water molecules and ions are not shown for transparency.

organized around the acyl chains of DLPC lipids exposing the lipid polar head groups to the solvent as reported from experimental observations.[18,19] The distribution of PMA-QA, in comparison to SMA-EA, surrounding the lipid tails were found to be distorted with few molecules localized on

the membrane surface (Fig. 2A). Atomistic inspection showed the N^+R_3 groups of the PMA-QA polymer were located close to (~ 5 to 7 Å) the anionic phosphate groups of DLPC lipids (Fig. 2A). A very strong hydrophobic lipid-polymer interaction is required to overcome the above-mentioned electrostatic polymer-lipid interaction (between N^+R_3 and PO_4^- groups) to uniformly assemble all the polymer molecules around the acyl chains of the lipid bilayer; this can be accomplished by enhancing the hydrophobicity of PMA-QA. In contrast, SMA-EA distribution was found to be uniform like a belt around DLPC acyl-chains (Fig.2B).

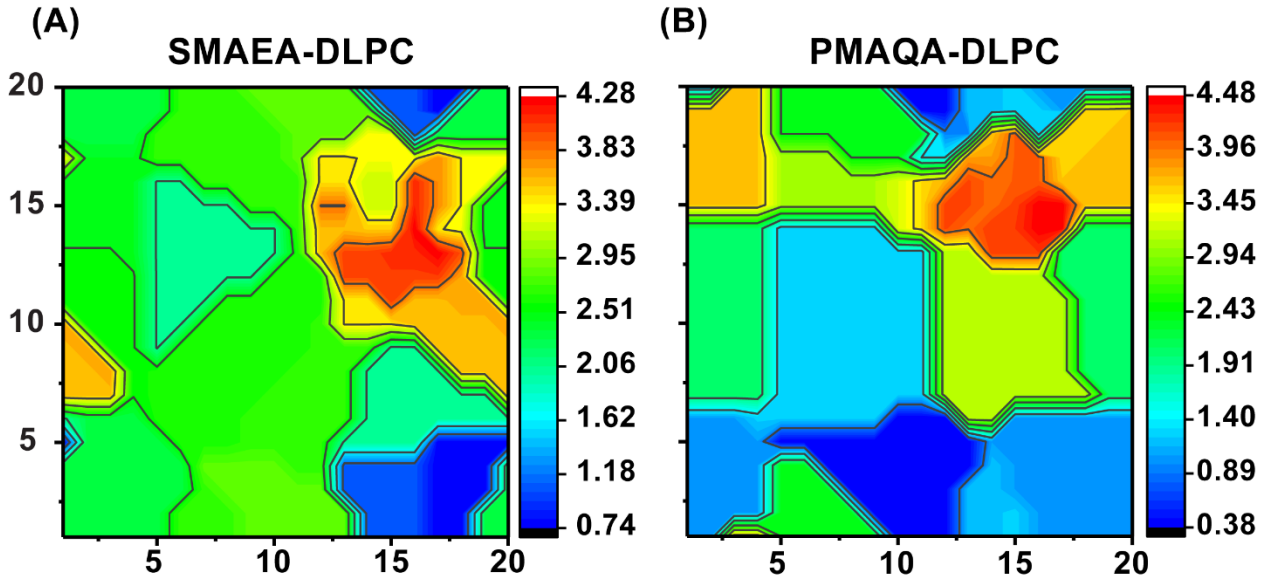

Figure 3. Lipid bilayer thickness in a polymer-encased DLPC nanodisc. The bilayer thickness is calculated from the final MD snapshot retrieved at 10 µs from SMA-EA-DLPC (A) and PMA-QA-DLPC (B) using *GriDMAT-MD*. It is plotted in a 20x20 matrix and the scale bar (in nm) is shown on the right.

Lipid bilayer thickness of a membrane mimetic plays a very important role on the membrane interaction, folding and topology of a membrane protein. Therefore, it is important to optimize the hydrophobic thickness of polymer based nanodiscs for a successful reconstitution of a membrane protein. While this is a daunting task to achieve experimentally, MD simulations can be used to test different parameters and provide guidelines for the design of a near-ideal polymer and optimized lipid composition to be used in a polymer nanodisc. Therefore, after successfully

monitoring the self-assembly process underlying the formation of lipid nanodiscs for two different polymers as described above (Fig.2), MD simulation results were used to analyze the influence of the orientations of polymer molecules in a nanodisc on the encased lipid-bilayer's thickness. As illustrated in Figure 3, SMA-EA nanodisc exhibited an average bilayer thickness of 25.4±1.5 Å as estimated from a 20x20 matrix using GridMAT-MD,[22] which is in agreement with the experimentally determined hydrophobic bilayer thickness of 24 Å for DLPC (Fig. 3A).[23] In addition, for a comparative analysis, we calculated the thickness of a membrane scaffold protein (MSP) encased DLPC nanodisc's lipid-bilayer generated using CHARMM_GUI[24] and it was found to be 32.9±2.6 Å (Fig. S3). On the other hand, the lipid bilayer surface distribution and random orientation of PAM-QA molecules exhibited a slightly lower average DLPC bilayer thickness (20.8±2.4 Å). In a PMA-QA-DLPC nanodisc, the thickness of several bilayer regions (blue regions in Fig.3B) was found to be <14 Å indicating a partial surface adsorption of PMA-QA molecules (Fig. 3B). A notable difference is the inhomogeneity of polymer-nanodiscs bilayer thickness when compared to the MSP-encased nanodiscs. This is due to the non-uniform stacking of polymer side-chains across the lipid acyl-chain unlike to the uniform and azimuthal alignment of the chains of two MSP proteins.[25–27] But, similar to MSP nanodiscs, polymer nanodiscs showed an edge effect on bilayer thickness along with a thicker center bilayer region.[26] However, an optimized membrane thickness for polymer nanodiscs may require longer time-scale of simulation to unify the edge effect of the polymer belt.

Since it is experimentally challenging to screen and optimize polymers and their lipid specificity to form stable nanodiscs, we examined the role of polymer's molecular size using MD simulation. Experimental results showed that PMA-QA with an optimal size of ~4.8 kDa forms nanodiscs.[18] Here, we tested the nanodisc-forming capability of ~4.8 kDa PMA-QA for a variable polymer:lipid

molar ratio as shown in Figure 4. At 1:8 PMA-QA:DLPC molar ratio, we observed spontaneous nanodisc formation with a uniform distribution of polymer molecules surrounding the hydrophobic acyl chains of DLPC lipids (Fig. 4A). Atomic inspection revealed that the hydrophobic butyl groups of the polymer are oriented toward the hydrophobic lipid core region, whereas the cationic $–N^+R_3$ groups of the polymer are exposed to the solvent (Fig. 4A). The ~ 4.8 kDa PMA-QA forms a DLPC nanodisc that is nearly equal to the size of SMA-EA nanodisc (~ 7.5 nm diameter). The ~ 4.8 kDa PMA-QA polymer nanodisc exhibited a non-uniform lipid-bilayer with an average thickness of 26.3 ±1.6 Å (Fig. 4C).

Next, we examined the effect of PMA-QA polymer concentration on the size and morphology of nanodiscs formed. An increase in the concentration of PMA-QA from 1:8 to a 1:4 molar ratio of PMA-QA:DLPC resulted in smaller size nanodisc as expected from previously reported experimental results; in addition, nanodiscs with average diameters of ~ 5.8, 5.0 and 3.5 nm were also observed (Fig. 4B). Unlike the PMA-QA nanodiscs obtained from ~4.8 kDa at a 1:8 PMA-QA:DLPC molar ratio (Fig. 4A), the nanodiscs formed at higher concentration of PMA-QA were found to contain PMA-QA in random orientations and tightly packed (Fig. 4B). Dynamic light scattering measurements of nanodiscs designed at a PMA-QA:DMPC molar ratio corresponding to that used in MD simulations supported the computationally observed nanodisc size mentioned above (Fig. 4D). As shown in Fig. 4D, the ~4.8 kDa PMA-QA at 1:8 polymer:DMPC molar ratio exhibited ~6.0 and ~ 7.7 nm size nanodiscs with a mass percentage of ~3.7 and 96.1%, respectively. On the other hand, for 1:4 PMA-QA:DMPC molar ratio, ~ 4.7, 6.0 and ~ 7.7 nm size nanodiscs with a mass percentage of ~ 7.2, 68.4 and 18.8%, respectively, were obtained (Fig. 4D).

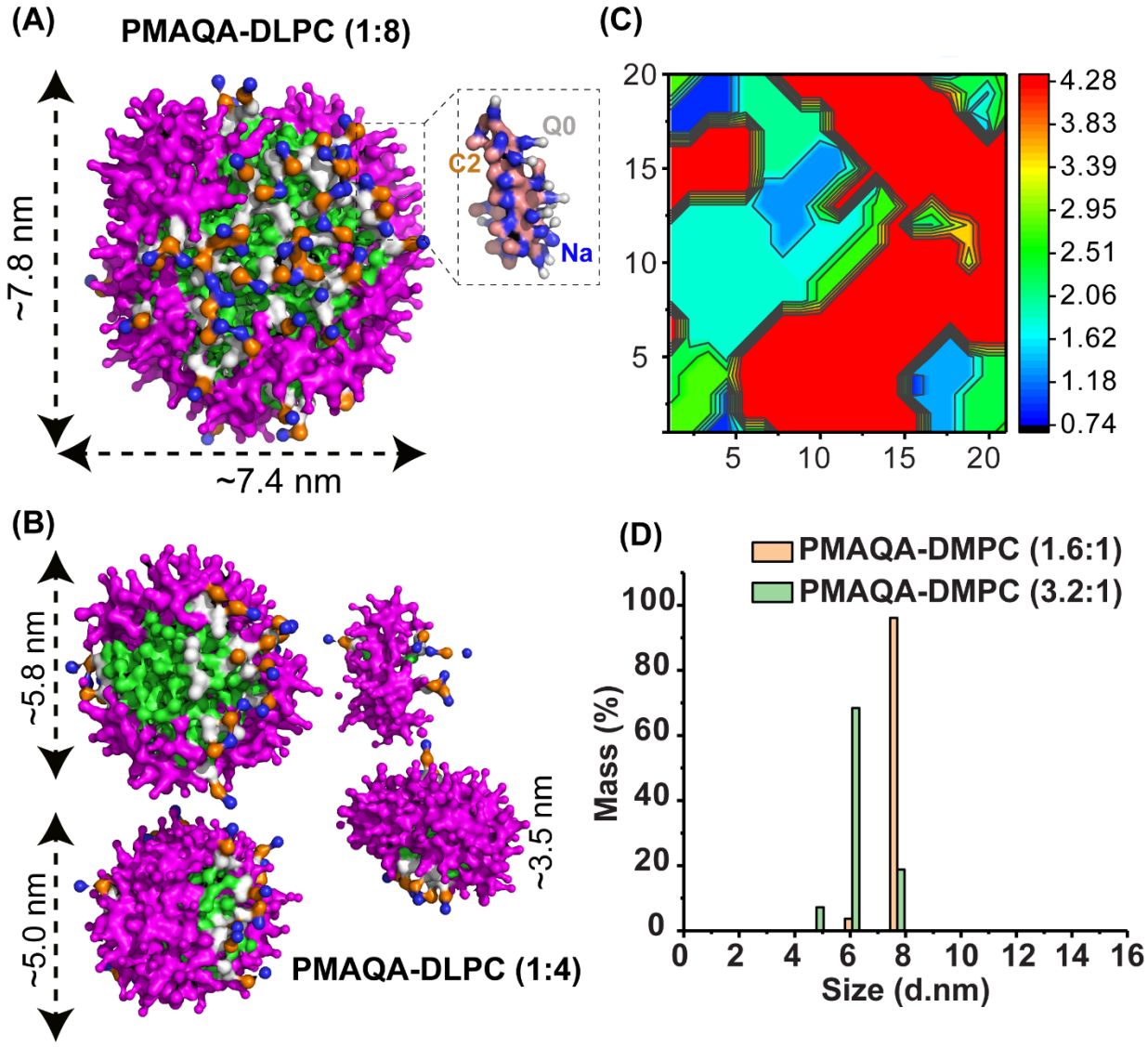

Figure 4. MD snapshots showing the formation of DLPC nanodisc by ~4.8 kDa PMA-QA at a variable polymer to lipid molar ratio. Spontaneous formation of nanodiscs by ~ 4.8 kDa PMA-QA at 1:8 (A) and 1:4 (B) polymer to DLPC molar ratio at 10 µs MD simulation. The polymers are shown in violet and DLPC atoms in different colors as indicated in Figure 2. Water molecules and ions are not shown for transparency. (C) Lipid-bilayer thickness calculated using GridMAT-MD from the MD snapshot shown in (A) is presented in a 20x20 matrix. The scale of thickness is shown on the right. (D) Dynamic light scattering showing the size distribution of PMA-QA-DLPC nanodiscs at the indicated polymer to lipid molar ratio.

MD simulation results (Fig.4) show that the lateral packing of lipids in PMA-QA nanodiscs depends on the size and concentration of the polymer as expected from experimental results.[18] The ability of MD simulations to reveal the location of different molecules constituting the nanodisc

can be utilized in the optimization of experimental conditions to achieve 'fluid lamellar phase' like lipid packing which is crucial for functional reconstitution of a membrane protein or a protein-protein complex[14]. Since experimental studies have reported the difficulties in reconstituting various lipid composition in polymer nanodiscs,[18,19] it is important to examine the suitability of the lipid composition for a given polymer to form stable nanodiscs using MD simulations. For this purpose, we simulated the self-assembly of PMA-QA or SMA-EA polymers in presence of anionic DLPS lipids (with DLPC acyl chains). As shown in Fig. S4, SMA-EA forms a nanodisc within a time-scale of 10 μs, whereas PMA-QA was found to be distributed on the membrane surface facilitated by its electrostatic interaction with negatively charged DLPS head groups.

Thermal stability of nanodiscs is important for various applications including the biophysical and structural studies of membrane proteins[28,29]. Experimental studies have reported that peptide or membrane scaffold protein based nanodiscs can be stable up to ~ 60 ˚C.[30] Thermal unfolding has been seen with further increase in temperature that destabilizes the nanodisc's size. In contrast to this, polymer-based nanodiscs are very stable and do not unfold even at 80˚ C.[19] To better understand the thermal stability of polymer based nanodiscs, we investigated the thermal stability of PMA-QA and SMA-EA-DLPC based nanodiscs with respect to temperature increasing from ~25 to ~140 ˚C as shown in Figure 5A. The simulated annealing experiment showed a minimal effect on the discoidal shape of polymer-nanodiscs with respect to temperature (Figure 5C,D). Quantitative analysis of the polymer-nanodisc size showed an average Feret's diameter of 8.05±0.24 nm for PMA-QA (8.46 nm at t=0μs) and 7.90±0.15 nm for SMA-EA-DLPC (8.02 nm at t=0μs) nanodiscs (Figure 5B). At a temperature range of ~37-80 ˚C, where the peptide or protein based nanodiscs unfold, both PMA-QA and SMA-EA nanodiscs exhibited stability as shown in

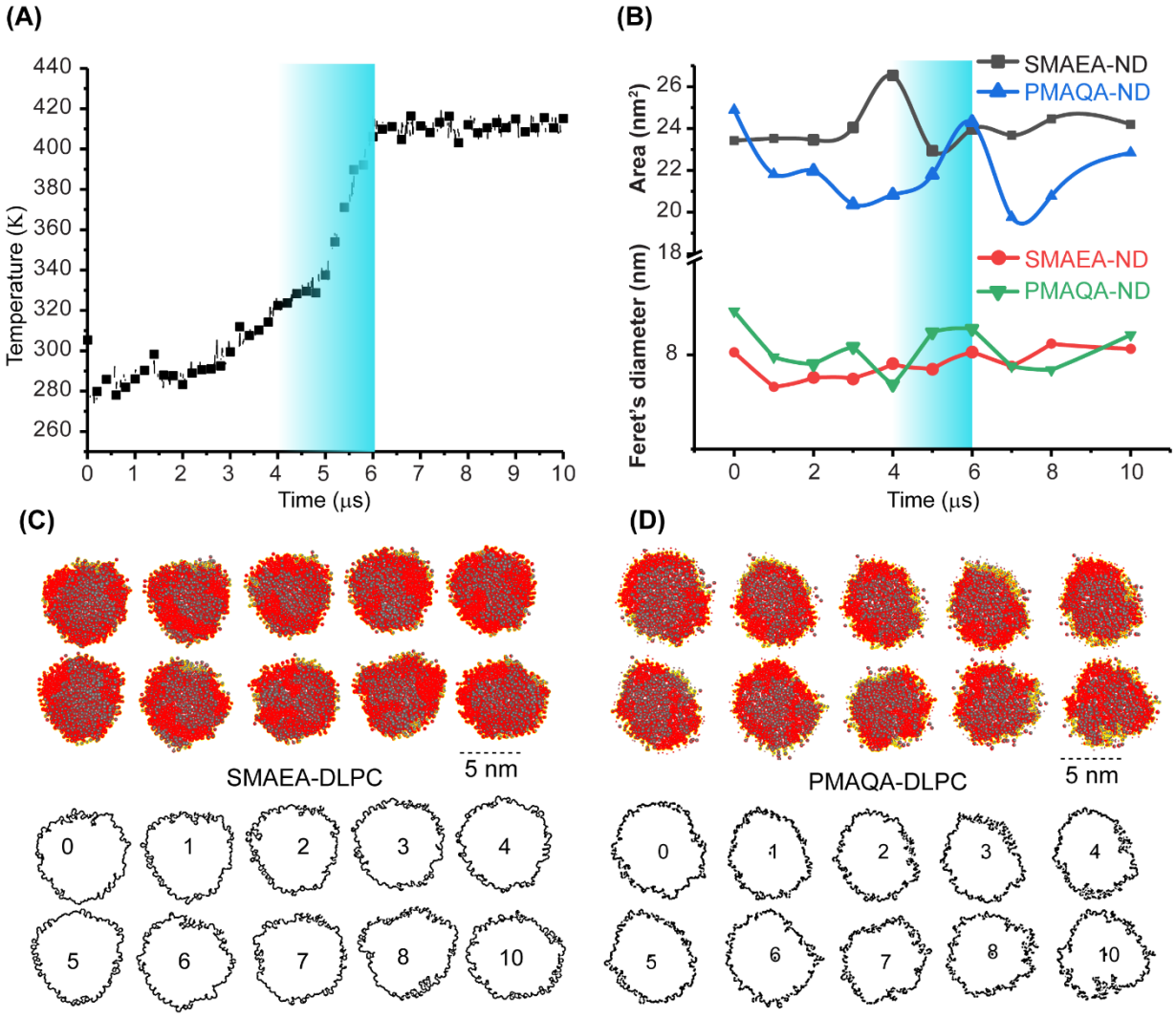

Figure 5. Thermal stability of SMA-EA or PMA-QA DLPC nanodiscs studied using simulated annealing MD simulation. (A) Polymer nanodiscs were subjected to a gradual increase in temperature from 298 to 415 K with respect to MD simulation time. (B) Feret's diameter and area of nanodiscs calculated from MD snapshots retrieved from 1μs time interval using ImageJ. The highlighted regions in (A) and (B) show the variation in nanodisc size and shape with respect to temperature. (C and D) Illustration of polymer-nanodiscs analyzed using *ImageJ* (red) and the distribution of polymer-belt as a function of indicated simulation times (in μs). The scale for ImageJ analysis is shown in dashed line.

Figure 5C and D. An average area of 21.93±1.66 nm^2 and 24.02±0.98 nm^2 was calculated from MD snapshots taken at 1μs interval of time for PMA-QA (24.88 nm^2 at t=0 μs) and SMA-EA-DLPC (23.42 nm^2 at t=0 μs) nanodiscs, respectively (Figure 5B). Overall, the simulated annealing MD simulation revealed the thermal stability of polymer nanodiscs above 80 ˚C.

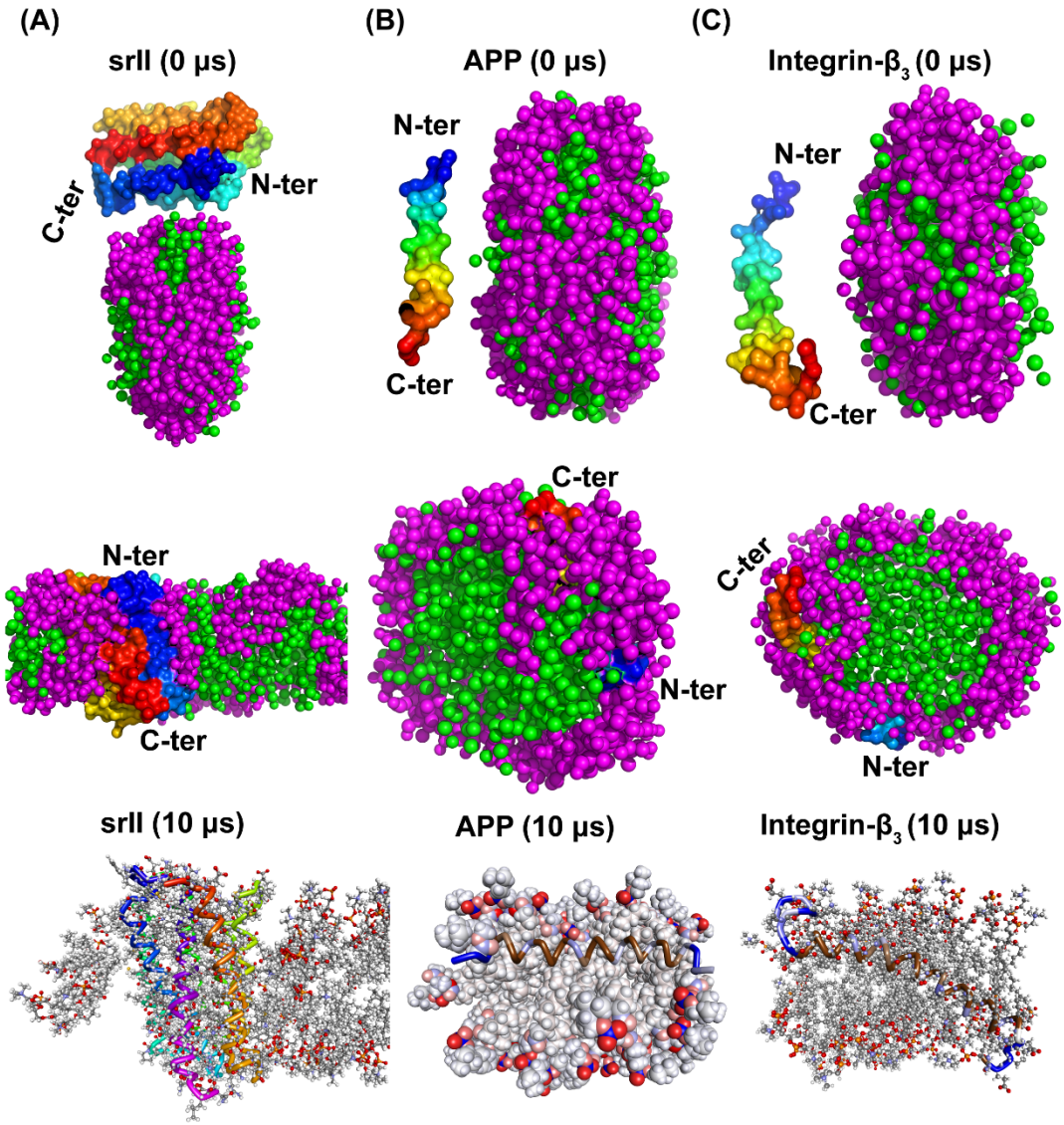

Figure 6. MD snapshots showing the reconstitution of membrane proteins in a SMA-EA-DLPC nanodisc. Monitoring the reconstitution of seven transmembrane domain sensory rhodopsin (A), single-pass transmembrane amyloid-precursor peptide (B) and integrin-β_3 (C) into a SMA-EA nanodisc (shown in Fig. 2B) using 5 μs CG MD. Polymers are shown in violet and DLPC atoms in green. The protein molecule is shown as spectrum in PyMOL with N- and C-termini (denoted as N-ter and C-ter) in blue and red, respectively. The initial (top row) and final (middle row) orientations of membrane proteins are shown. The Martini CG to all-atom conversion models are shown in the bottom-most row. Membrane proteins are shown in ribbon and lipids in ball-stick or CPK. Zoomed structure of all-atom model structures are given in Supplementary Figures S6 and S7.

Next, we studied the spontaneous reconstitution of a seven transmembrane domain bacterial sensory rhodopsin (srII) (PDB ID: 1XIO)[31], and single transmembrane containing membrane

proteins like integrin-β_3 (PDB ID: 2L91)[17] and amyloid precursor protein (APP) (PDB ID: 2LLM)[32] in polymer nanodiscs. Membrane proteins were initially placed ~ 1 nm away from the SMEA-DLPC nanodisc as shown in Figure. 6A. The srII protein was found to interact with the edge of the nanodisc (SMA-EA belt). The complex remained stable for several microseconds (~1 μs) followed by a change in the shape of the nanodisc from a discoidal to ellipsoidal shape (Fig. S5). The lipid bilayer insertion of srII at 4 μs displaced several of SMA-EA polymer molecules, and from 6 to 8 μs the seven transmembrane domains of the protein gradually oriented perpendicular to the plane of the lipid-bilayer (Fig. S5). CG to all-atom conversion showed that the srII transmembrane domains were well oriented within the lipid-bilayer;[15] however, the ~7.5 nm size nanodisc was found to be not efficient in maintaining the discoidal shaped structural integrity of SMA-EA-DLPC nanodisc (Figs. 6A and S5).

We then studied the reconstitution of two different single-pass transmembrane proteins, namely APP and integrin-β_3 (Fig. 6B,C). Remarkably, unlike srII, APP and integrin-β_3 were found to have little effect on the shape and size of SMA-EA nanodiscs. Both APP and integrin-β_3 were found to interact with nanodiscs within several nanoseconds and interact with the polymer belt. APP fragment was found to align at angle ~ 90° with respect to the nanodisc's lipid-bilayer normal similar to apolipoprotein mimetic peptides (Fig. S6) and sit close to the edge of nanodisc as a peptide belt (Fig. 6B).[33] On the other hand, integrin-β_3 was found to localize in the lipid-bilayer with ~ 30° tilt of the C-terminus transmembrane helix with respect to the lipid-bilayer normal, which is in agreement with the reported experimental observation[17] (Fig. S7).

In conclusion, we have successfully demonstrated the formation of lipid-nanodiscs by two different amphiphilic copolymers consisting of styrene or polymethacrylate moieties using atomistic CG MD simulation. We expect that the parametrization of the polymers and

methodology presented in this study will be useful in designing and screening new polymers that can efficiently form nanodiscs. The optimization of polymer length, lipid specificity and stability would not only provide a better understanding of the polymer-belt interference with the target membrane protein and its function, but also be useful in the development of nanomedicine or peptide membrane interaction studies as demonstrated in this work.[13] We foresee that the computational approach employed here can be generalized by varying the polymer hydrophobic and hydrophilic moieties to design membrane protein selective nanodisc systems for a successful reconstitution. The coarse-grained parameters optimized for Martini force-field framework in this study for polymers will create avenues for further development of coarse-grained systems for other polymers to be used in biological and chemical studies.

ASSOCIATED CONTENT

Supporting Information

Detailed methods, Table listing the molecular dynamics parameters, lipid-bilayer pore formation by SMA-EA, initial distribution of polymer and lipid, membrane scaffold protein nanodisc, DLPS nanodiscs formation by PMA-QA and SMA-EA, time interval sensory rhodopsin translation reconstituted in SMA-EA-DLPC nanodiscs, coarse-grained to all-atom conversion

AUTHOR INFORMATION

Corresponding Author

*E-mail: ramamoor@umich.edu

Notes

The authors declare no competing financial interest.

ACKNOWLEDGMENT

This study was supported by funds from NIH (AG048934 to A.R.). We thank Dr. Charles L. Brooks III for fruitful discussion on the use of molecular dynamics simulations to study nanodiscs. This work was (in part) performed under the International Collaborative Research Program of Institute for Protein Research, Osaka University, ICR-18-02. We thank Professor Toshimichi Fujiwara in the Institute for Protein Research, Osaka University, for providing parallel computing facility on *SGI* UV 3000.

REFERENCES

(1) Zorman, S.; Botte, M.; Jiang, Q.; Collinson, I.; Schaffitzel, C. Advances and Challenges of Membrane-Protein Complex Production. *Curr. Opin. Struct. Biol.* **2015**, *32*, 123–130.

(2) Carpenter, E. P.; Beis, K.; Cameron, A. D.; Iwata, S. Overcoming the Challenges of Membrane Protein Crystallography. *Curr. Opin. Struct. Biol.* **2008**, *18* (5), 581–586.

(3) Kucik, D. F.; Elson, E. L.; Sheetz, M. P. Weak Dependence of Mobility of Membrane Protein Aggregates on Aggregate Size Supports a Viscous Model of Retardation of Diffusion. *Biophys. J.* **1999**, *76* (1 I), 314–322.

(4) Frey, L.; Lakomek, N. A.; Riek, R.; Bibow, S. Micelles, Bicelles, and Nanodiscs: Comparing the Impact of Membrane Mimetics on Membrane Protein Backbone Dynamics. *Angew. Chemie - Int. Ed.* **2017**, *56* (1), 380–383.

(5) Denisov, I. G.; Sligar, S. G. Nanodiscs in Membrane Biochemistry and Biophysics. *Chem. Rev.* **2017**, *117* (6), 4669–4713.

(6) Barnaba, C.; Sahoo, B. R.; Ravula, T.; Medina-Meza, I. G.; Im, S.-C.; Anantharamaiah, G. M.; Waskell, L.; Ramamoorthy, A. Cytochrome-P450-Induced Ordering of Microsomal Membranes Modulates Affinity for Drugs. *Angew. Chemie - Int. Ed.* **2018**, *35294*, 3391–3395.

(7) Song, Q.; Huang, M.; Yao, L.; Wang, X.; Gu, X.; Chen, J.; Chen, J.; Huang, J.; Hu, Q.; Kang, T.; et al. Lipoprotein-Based Nanoparticles Rescue the Memory Loss of Mice with Alzheimer's Disease by Accelerating the Clearance of Amyloid-Beta. *ACS Nano* **2014**, *8* (3), 2345–2359.

(8) Song, H.; Ma, X.; Xu, J.; Song, Q.; Hu, M.; Gu, X.; Zhang, Q.; Hou, L.; Chen, L.; Huang, Y.; et al. The Shape Effect of Reconstituted High-Density Lipoprotein Nanocarriers on Brain Delivery and Aβ Clearance. *Nano Res.* **2018**, 1–14.

(9) Sahoo, B. R.; Genjo, T.; Cox, S. J.; Stoddard, A. K.; Anantharamaiah, G. M.; Fierke, C.; Ramamoorthy, A. Nanodisc-Forming Scaffold Protein Promoted Retardation of Amyloid-Beta Aggregation. *J. Mol. Biol.* **2018**.

(10) Hagn, F.; Etzkorn, M.; Raschle, T.; Wagner, G. Optimized Phospholipid Bilayer Nanodiscs Facilitate High-Resolution Structure Determination of Membrane Proteins. *J. Am. Chem. Soc.* **2013**, *135* (5), 1919–1925.

(11) Fiori, M. C.; Jiang, Y.; Zheng, W.; Anzaldua, M.; Borgnia, M. J.; Altenberg, G. A.; Liang, H. Polymer Nanodiscs: Discoidal Amphiphilic Block Copolymer Membranes as a New Platform for Membrane Proteins. *Sci. Rep.* **2017**, *7* (1), 1–9.

(12) Dörr, J. M.; Scheidelaar, S.; Koorengevel, M. C.; Dominguez, J. J.; Schäfer, M.; van Walree, C. A.; Killian, J. A. The Styrene–maleic Acid Copolymer: A Versatile Tool in Membrane Research. *Eur. Biophys. J.* **2016**, *45* (1), 3–21.

(13) Sahoo, B.; Genjo, T.; Bekier II, M.; Cox, S. N.; Stoddard, A.; Ivanova, M.; Yasuhara, K.; Fierke,

C.; Wang, Y.; Ramamoorthy, A. Alzheimer's Amyloid-Beta Intermediates Generated by Polymer-Nanodiscs. *Chem. Commun.* **2018**.

(14) Ravula, T.; Hardin, N.; Bai, J.; Im, S.-C.; Waskell, L.; Ramamoorthy, A. Effect of Polymer Charge on Functional Reconstitution of Membrane Proteins in Polymer Nanodiscs. *Chem. Commun.* **2018**.

(15) Sahoo, B. R.; Fujiwara, T. Conformational States of HAMP Domains Interacting with Sensory Rhodopsin Membrane Systems: An Integrated All-Atom and Coarse-Grained Molecular Dynamics Simulation Approach. *Mol. Biosyst.* **2017**, *13* (1), 193–207.

(16) Pantelopulos, G. A.; Straub, J. E.; Thirumalai, D.; Sugita, Y. Structure of APP-C991–99and Implications for Role of Extra-Membrane Domains in Function and Oligomerization. *Biochim. Biophys. Acta - Biomembr.* **2018**, *1860* (9), 1698–1708.

(17) Kim, C.; Schmidt, T.; Cho, E. G.; Ye, F.; Ulmer, T. S.; Ginsberg, M. H. Basic Amino-Acid Side Chains Regulate Transmembrane Integrin Signalling. *Nature* **2012**, *481* (7380), 209–214.

(18) Yasuhara, K.; Arakida, J.; Ravula, T.; Ramadugu, S. K.; Sahoo, B.; Kikuchi, J. I.; Ramamoorthy, A. Spontaneous Lipid Nanodisc Fomation by Amphiphilic Polymethacrylate Copolymers. *J. Am. Chem. Soc.* **2017**, *139* (51), 18657–18663.

(19) Ravula, T.; Ramadugu, S. K.; Di Mauro, G.; Ramamoorthy, A. Bioinspired, Size-Tunable Self-Assembly of Polymer–Lipid Bilayer Nanodiscs. *Angew. Chemie - Int. Ed.* **2017**, *56* (38), 11466–11470.

(20) De Jong, D. H.; Singh, G.; Bennett, W. F. D.; Arnarez, C.; Wassenaar, T. A.; Schäfer, L. V.; Periole, X.; Tieleman, D. P.; Marrink, S. J. Improved Parameters for the Martini Coarse-Grained Protein Force Field. *J. Chem. Theory Comput.* **2013**, *9* (1), 687–697.

(21) Xue, M.; Cheng, L.; Faustino, I.; Guo, W.; Marrink, S. J. Molecular Mechanism of Lipid Nanodisc Formation by Styrene Maleic Acid Copolymers. *Biophys. J.* **2018**, *0* (0), 1–9.

(22) Allen, W. J.; Lemkul, J. a.; Bevan, D. R. GridMAT-MD: A Grid-Based Membrane Analysis Tool for Use with Molecular Dynamics. *J Comput Chem* **2009**, *30* (12), 1952–1958.

(23) Skar-Gislinge, N.; Simonsen, J. B.; Mortensen, K.; Feidenhans'l, R.; Sligar, S. G.; Lindberg Møller, B.; Bjørnholm, T.; Arleth, L. Elliptical Structure of Phospholipid Bilayer Nanodiscs Encapsulated by Scaffold Proteins: Casting the Roles of the Lipids and the Protein. *J. Am. Chem. Soc.* **2010**, *132* (39), 13713–13722.

(24) Jo, S.; Kim, T.; Iyer, V. G.; Im, W. CHARMM-GUI: A Web-Based Graphical User Interface for CHARMM. *J. Comput. Chem.* **2008**, *29* (11), 1859–1865.

(25) Siuda, I.; Tieleman, D. P. Molecular Models of Nanodiscs. *J. Chem. Theory Comput.* **2015**, *11* (10), 4923–4932.

(26) Schuler, M. A.; Denisov, I. G.; Sligar, S. G. Nanodiscs as a New Tool to Examine Lipid-Protein Interactions. *Methods Mol. Biol.* **2013**, *974*, 415–433.

(27) Debnath, A.; Schäfer, L. V. Structure and Dynamics of Phospholipid Nanodiscs from All-Atom and Coarse-Grained Simulations. *J. Phys. Chem. B* **2015**, *119* (23), 6991–7002.

(28) Nasr, M. L.; Baptista, D.; Strauss, M.; Sun, Z. J.; Grigoriu, S.; Huser, S.; Plückthun, A.; Hagn, F.; Walz, T.; Hogle, J. M.; et al. Proteins and Viral Entry. **2018**, *14* (1), 49–52.

(29) Wadsäter, M.; Maric, S.; Simonsen, J. B.; Mortensen, K.; Cardenas, M. The Effect of Using Binary Mixtures of Zwitterionic and Charged Lipids on Nanodisc Formation and Stability. *Soft Matter* **2013**, *9* (7), 2329–2337.

(30) Kariyazono, H.; Nadai, R.; Miyajima, R.; Takechi-Haraya, Y.; Baba, T.; Shigenaga, A.; Okuhira, K.; Otaka, A.; Saito, H. Formation of Stable Nanodiscs by Bihelical Apolipoprotein A-I Mimetic Peptide. *J. Pept. Sci.* **2016**, *22* (2), 116–122.

(31) Vogeley, L.; Sineshchekov, O. A.; Trivedi, V. D.; Sasaki, J.; Spudich, J. L.; Luecke, H. Anabaena Sensory Rhodopsin: A Photochromic Color Sensor at 2.0 Å. *Science (80-.).* **2004**, *306* (5700), 1390–1393.

(32) Nadezhdin, K. D.; Bocharova, O. V; Bocharov, E. V; Arseniev, A. S. Structural and Dynamic Study of the Transmembrane Domain of the Amyloid Precursor Protein. *Acta Naturae* **2011**, *3* (1), 69–76.

(33) Pourmousa, M.; Pastor, R. W. Molecular Dynamics Simulations of Lipid Nanodiscs. *Biochim.*

Biophys. Acta - Biomembr. **2018**, No. December 2017, 0–1.